

Marquette University
e-Publications@Marquette

Chemistry Faculty Research and Publications

Chemistry, Department of

1-29-2014

The Active Site Sulfenic Acid Ligand in Nitrile Hydratases Can Function as a Nucleophile

Salette Martinez
Loyola University Chicago

Rui Wu
Loyola University Chicago

Ruslan Sanishvili
Argonne National Laboratory

Dali Liu
Loyola University Chicago

Richard C. Holz
Marquette University, richard.holz@marquette.edu

Published version. *Journal of the American Chemical Society*, Vol. 136, No. 4 (January 29, 2014): 1186-1189. DOI. © 2014 American Chemical Society. Used with permission.
ACS AuthorChoice - This is an open access article published under an ACS AuthorChoice License, which permits copying and redistribution of the article or any adaptations for non-commercial purposes.



The Active Site Sulfenic Acid Ligand in Nitrile Hydratases Can Function as a Nucleophile

Salette Martinez,^{†,‡,⊥} Rui Wu,^{‡,⊥} Ruslan Sanishvili,[§] Dali Liu,[‡] and Richard Holz^{*,†}

[†]Department of Chemistry, Marquette University, Milwaukee, Wisconsin 53201, United States

[‡]Department of Chemistry and Biochemistry, Loyola University Chicago, Chicago, Illinois 60660, United States

[§]X-ray Science Division, Advanced Photon Source, Argonne National Laboratory, 9700 South Cass Avenue, Lemont, Illinois 60439, United States

S Supporting Information

ABSTRACT: Nitrile hydratase (NHase) catalyzes the hydration of nitriles to their corresponding commercially valuable amides at ambient temperatures and physiological pH. Several reaction mechanisms have been proposed for NHase enzymes; however, the source of the nucleophile remains a mystery. Boronic acids have been shown to be potent inhibitors of numerous hydrolytic enzymes due to the open shell of boron, which allows it to expand from a trigonal planar (sp^2) form to a tetrahedral form (sp^3). Therefore, we examined the inhibition of the Co-type NHase from *Pseudonocardia thermophila* JCM 3095 (PtNHase) by boronic acids via kinetics and X-ray crystallography. Both 1-butaneboronic acid (BuBA) and phenylboronic acid (PBA) function as potent competitive inhibitors of PtNHase. X-ray crystal structures for BuBA and PBA complexed to PtNHase were solved and refined at 1.5, 1.6, and 1.2 Å resolution. The resulting PtNHase–boronic acid complexes represent a “snapshot” of reaction intermediates and implicate the cysteine-sulfenic acid ligand as the catalytic nucleophile, a heretofore unknown role for the α Cys¹¹³–OH sulfenic acid ligand. Based on these data, a new mechanism of action for the hydration of nitriles by NHase is presented.

Nitrile hydratase (NHase, E.C. 4.2.1.84) is a metalloenzyme within the nitrile degradation pathway that catalyzes the hydration of nitriles to their corresponding amides under mild conditions (room temperature and physiological pH).^{1,2} NHases consist of two nonhomologous subunits, α and β , that form $\alpha_2\beta_2$ heterotetramers.^{3–6} Several NHases have been structurally characterized and shown to contain either a low-spin nonheme Fe(III) ion (Fe-type) or a low-spin noncorrin Co(III) ion (Co-type) in their active site. The metal ion is coordinated by three cysteine sulfur atoms, two amide nitrogens, and a water molecule.⁷ Two of the active site cysteine residues are post-translationally modified to cysteine-sulfenic acid (Cys–SO₂H) and cysteine-sulfenic acid (Cys–SOH) yielding an unusual metal coordination geometry, termed a “claw setting”.⁷ NHases have attracted substantial interest as biocatalysts in preparative organic chemistry and are used in several industrial applications such as the large scale production of acrylamide and nicotinamide.^{8,9} In addition, because of their exquisite reaction specificity, the nitrile-

hydrolyzing potential of NHases is becoming increasingly recognized as a new type of “green” chemistry for the degradation of environmentally harmful nitriles such as bromoxynil, a nitrile-based pesticide.¹⁰

Several reaction mechanisms have been proposed for NHase enzymes; however, the precise catalytic pathway remains elusive. Based on single turnover stopped-flow data, the nitrile substrate nitrogen was shown to bind directly to the active site metal ion displacing the axial water molecule.¹¹ Once bound, imidate is likely formed as the result of nucleophilic attack, which then isomerizes to the corresponding amide. However, the source of the nucleophile for this transformation is still under debate. To gain insight into the identity of the active site nucleophile, we examined the inhibition of the Co-type NHase from *Pseudonocardia thermophila* JCM 3095 (PtNHase) by boronic acids. The resulting X-ray crystal structures of PtNHase–boronic acid complexes are a “snapshot” of potential reaction intermediates and implicate the cysteine-sulfenic acid ligand as the catalytic nucleophile. The combination of these data with previously reported spectroscopic and X-ray crystallographic data have allowed a novel mechanism of action to be proposed for the metal-mediated nitrile hydration reaction catalyzed by NHase enzymes.

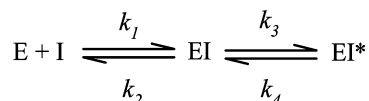
The ability of both 1-butaneboronic acid (BuBA) and phenylboronic acid (PBA) to inhibit PtNHase was examined by monitoring the hydration of acrylonitrile to acrylamide spectrophotometrically at 225 nm ($\epsilon = 2.9 \text{ mM}^{-1} \text{ cm}^{-1}$). In the absence of inhibitors, PtNHase catalyzed the hydration of acrylonitrile at pH 7.5 and 25 °C with a k_{cat} value of $1310 \pm 110 \text{ s}^{-1}$ and a K_{m} value of $0.8 \pm 0.1 \text{ mM}$. Inspection of the reaction time course for the hydration of acrylonitrile at pH 7.5 and 25 °C by PtNHase in the presence of BuBA or PBA indicates that both boronic acids function as potent competitive inhibitors of PtNHase. For BuBA, linear reaction progress curves were observed providing an inhibition constant (K_i) of $0.5 \pm 0.1 \mu\text{M}$. On the other hand, PBA displayed biphasic progress curves, which is characteristic of slow-binding inhibition (Figure S1).¹²

The slow-binding inhibition properties of PBA were analyzed based on the equilibrium shown in Scheme 1, where K_i ($K_i = k_1/k_2$) is the equilibrium inhibition constant for the formation

Received: October 11, 2013

Published: January 2, 2014

Scheme 1



of the initial complex, EI, and k_3 and k_4 are the forward and reverse rate constants for the equilibrium between the EI and the EI* complex.¹² By measuring the reaction time course at different concentrations of PBA and substrate, the initial K_i was found to be $5.0 \pm 0.9 \mu\text{M}$. The overall K_i^* of $0.04 \pm 0.01 \text{ nM}$, where $K_i^* = K_i k_4 / (k_3 + k_4)$, was determined by preincubating PtNHase with PBA for 1 h at pH 7.5 and 25 °C followed by reaction with various concentrations of acrylonitrile.

Since both BuBA and PBA function as competitive inhibitors of PtNHase, they must bind to the enzyme active site. In solution, BuBA was reported to be >99% in the boronic acid form (sp^2 hybridized) at pH 8.0, with a reported pK_a of 10.6.¹³ Similarly, the pK_a of PBA is 8.9,¹⁴ so it too will be in the boronic acid form at pH 7.5. Therefore, both BuBA and PBA likely bind to PtNHase in their sp^2 hybridized forms resulting in the displacement of the axial water molecule. This initial Co(III) binding step was hypothesized to be followed by attack of an active site nucleophile, such as the sulfenic acid ligand, on the electron deficient p_z orbital of the boron atom, since it was recently suggested that boronic acids might inhibit NHases by interacting with the sulfenic acid ligand.¹⁵ Nucleophilic attack of the electron-deficient p_z orbital of the boron atom is also consistent with previous studies of boronic acid inhibitors bound to hydrolytic enzymes, as hydrolytic reactions typically proceed through a transition state resulting from nucleophilic attack of the substrate.^{16,17}

To confirm that BuBA binds directly to the low-spin Co(III) ion in the active site of PtNHase and to determine if BuBA has undergone nucleophilic attack, X-ray crystal structures of wild-type (WT) PtNHase and two PtNHase–BuBA complexes formed by either soaking or cocrystallization were solved and refined to 1.9, 1.5, and 1.6 Å resolution, respectively. Details of the data collection and refinement statistics are given in Table S1 of the Supporting Information (SI). The overall structure of WT PtNHase is identical to the previously reported structure (PDB code: 1IRE).¹⁸ The active site is the typical “claw setting” observed in all nitrile hydratases with an axial water molecule that forms hydrogen bonds with αSer^{112} , the sulfenic acid ligand ($\alpha\text{Cys}^{111}\text{--O}_2\text{H}$), and the sulfenic acid ligand ($\alpha\text{Cys}^{113}\text{--OH}$). The protonation states of the sulfenic and sulfenic acid ligands have previously been assigned based on sulfur K-edge XAS data, which indicated the presence of three types of Cys ligands in a WT Fe-type NHase.¹⁹ These XAS data combined with geometry-optimized DFT calculations suggested the presence of CysS^- , CysSOH , and CysSO_2^- at pH 7.5.

Upon soaking a crystal of WT PtNHase in cryo-protectant containing 10 mM BuBA for 20 s followed by flash freezing in liquid nitrogen, electron density corresponding to the boronic acid inhibitor was present at the active site replacing the axial water molecule (Figure 1). This observation is consistent with the fact that BuBA is a competitive inhibitor of PtNHase. In the WT structure (not shown) the $\text{Co(III)--O}_{\text{water}}$ bond distance is 2.3 Å compared to a Co(III)--O boronic acid oxygen bond distance of 2.2 Å. Interestingly, the O-atom of the sulfenic acid ligand ($\alpha\text{Cys}^{113}\text{--OH}$) is covalently bound to the boron atom of BuBA (1.5 Å) (Figure 1). This covalent bond, which has not been observed previously, is the result of nucleophilic attack of

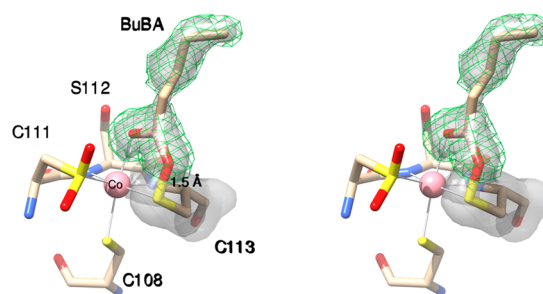


Figure 1. Stereoview of PtNHase bound by BuBA after soaking a crystal of WT PtNHase in cryo-protectant containing 10 mM BuBA for 20 s followed by flash freezing in liquid nitrogen. The $2f_o - f_c$ map is shown as a transparent gray surface at the 1.1σ level around BuBA and αCys^{113} . The simulated-annealing omit map ($f_o - f_c$) is shown around BuBA as a green mesh at 2.7σ .

the sulfenic acid O-atom on the empty p_z orbital of the B-atom and the subsequent loss of a boronic acid O-atom. Even though the O-atom of $\alpha\text{Cys}^{113}\text{--OH}$ is covalently bound to boron, αCys^{113} remains ligated to the low-spin Co(III) ion with a bond distance of 2.2 Å identical to that observed in the WT enzyme. The resulting B-atom is essentially trigonal planar (sp^2) with a dihedral angle of $\sim 170^\circ$.

On the other hand, the PtNHase–BuBA structure obtained via cocrystallization of WT PtNHase and 10 mM BuBA reveals that the S–O boronic acid oxygen interaction is significantly diminished (Figure 2). BuBA binding displaces the axial water

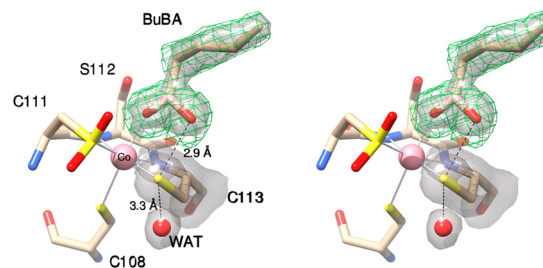


Figure 2. Stereoview of PtNHase bound by BuBA obtained via cocrystallization of WT PtNHase and 10 mM BuBA. The $2f_o - f_c$ map is shown as a transparent gray surface at the 1.1σ level around BuBA and αCys^{113} . The simulated-annealing omit map ($f_o - f_c$) is shown around BuBA as a green mesh at 2.8σ .

molecule resulting in a Co(III)--O bond distance of 2.2 Å; however, the second O-atom of BuBA is 2.9 Å away from the S-atom of Cys^{113} . While this distance is still within the van der Waals radii of S and O, which is $\sim 3.3 \text{ Å}$, it is clear that the $\alpha\text{Cys}^{113}\text{--OH}$ interaction is considerably weakened compared to that observed in the PtNHase–BuBA structure obtained via soaking. This weak S–O interaction is likely due to the initial dissociation of boronic acid from the active site and not the initial binding step. If it were the initial binding step of a boronic acid, αCys^{113} would need to be in its fully reduced form which is not the case, as αCys^{113} is clearly oxidized to its sulfenic acid form in the WT PtNHase structure. Therefore, the observed S–O elongation is assigned to boronic acid dissociation. The αCys^{113} sulfur remains bound to the Co(III) ion with a bond length of 2.3 Å. The B-atom of BuBA also remains nearly trigonal planar (sp^2) with a dihedral angle of $\sim 160^\circ$.

These two structures represent a “snapshot” of two potential intermediate states in nitrile hydration by depicting nucleophilic attack by the sulfenic acid ligand and the initial stage of the product-release step. Product loss may occur as the result of a concomitant nucleophilic attack on the αCys^{113} ligand by a water molecule. This is consistent with the observation that a water molecule that is H-bound (2.9 Å) to the NH_2 group of βArg^{157} is only 3.3 Å from the αCys^{113} ligand. This water molecule may represent the incoming O-atom required to reestablish the $\alpha\text{Cys}^{113}\text{-OH}$ ligand. Interestingly, no water molecule is observed within 4 Å of the B-atom in either BuBA structure (Figure 2), suggesting that a water molecule is not poised for nucleophilic attack on the B-atom facilitating boronic acid formation and product release.

Since *PtNHase* can hydrate both alkyl and aromatic nitriles,¹⁸ the X-ray crystal structure of the *PtNHase*-PBA complex also was obtained via cocrystallization of WT *PtNHase* and 10 mM PBA and refined to 1.2 Å resolution (Figures 3 and S2). Details

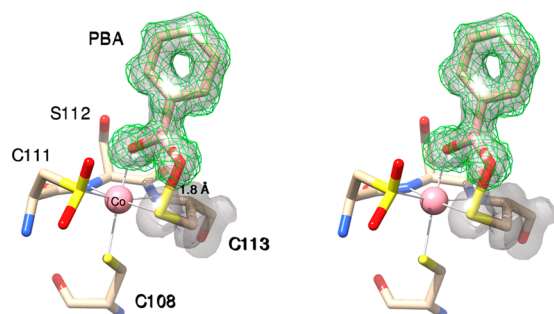


Figure 3. Stereoview of *PtNHase* bound by PBA at 1.2 Å resolution obtained via cocrystallization of WT *PtNHase* and 10 mM PBA. The $2f_o - f_c$ map of the structural model representing 80% occupancy is shown as a transparent gray surface at the 1.4 σ level around PBA and αCys^{113} . The simulated-annealing omit map ($f_o - f_c$) is shown around PBA as a green mesh at 2.8 σ .

of data collection and refinement statistics are given in Table S1 of the SI. Interestingly, electron density corresponding to the active site cobalt ion and the PBA suggests $\sim 80\%$ occupancy. These data are consistent with inductively coupled atomic emission spectroscopy (ICP-AES), which typically indicates that only 0.8 to 0.9 cobalt ions are present per $\alpha\beta$ dimer. Similar to the *PtNHase*-BuBA structure obtained via soaking, the structural model representing 80% occupancy contains a boronic acid O-atom that displaces the axial water molecule and binds directly to the active site Co(III) ion with a bond distance of 2.2 Å (Figures 3 and S2). Similar to the *PtNHase*-BuBA structure (Figure 1), the B-atom of PBA has undergone nucleophilic attack by the $\alpha\text{Cys}^{113}\text{-OH}$ O-atom forming a covalent bond with a B-O distance of 1.5 Å and a S-O bond distance of 1.8 Å. The S-atom of $\alpha\text{Cys}^{113}\text{-OH}$ remains a Co(III) ligand with a bond distance of 2.2 Å. The resulting B-atom is nearly trigonal planar with a dihedral angle of $\sim 160^\circ$, and the unbound O-atom of the original boronic acid moiety is lost. The structural model representing the remaining $\sim 20\%$ of the observed density is similar to the previously reported apo-*PtNHase* (Figure S2).¹⁸ These data indicate that the *PtNHase*-PBA complex represents a covalently bound intermediate state for nitrile hydration, similar to the *PtNHase*-BuBA complexes, where the $\alpha\text{Cys}^{113}\text{-OH}$ ligand functions as the nucleophile.

Based on the three structures reported herein, parallels can be drawn between boronic acid binding to *PtNHase* and a

nitrile substrate that are consistent with the sulfenic acid ligand functioning as a nucleophile. Kinetic and X-ray crystallographic data indicate that proper oxidation of the αCys^{113} ligand to a cysteine-sulfenic acid is essential for NHase enzymes to be active catalysts suggesting that the S-OH bond is polarized and poised for nucleophilic attack.^{20–22} The catalytic function of the $\alpha\text{Cys}^{113}\text{-OH}$ is also consistent with the rate constants provided by single-turnover stopped-flow studies that indicate a fast pseudo-first-order step that involves substrate binding to the trivalent metal ion in the enzyme active site, while product release is the rate-limiting step consistent with a sulfenic acid covalent intermediate complex.¹¹ Additional evidence for metal-ligated sulfenic acids that can function as nucleophiles can be gleaned from NHase model complex studies.^{23–25} A coordinatively saturated bis(sulfenato-S)Co(III) complex was shown to slowly hydrate acetonitrile to acetamide under acidic conditions while the bis(sulfinato)Co(III) complex was unable to hydrate nitriles. As neither of these compounds have an open coordination site to allow nitrile or water binding, these data implicated the Co(III) sulfenic acid ligand as the nucleophile.

In conclusion, it has long been assumed that a water molecule or a hydroxide ion in the NHase active site functions in the initial nucleophilic attack on an activated nitrile C-atom. However, in this work we present evidence that the $\alpha\text{Cys}^{113}\text{-OH}$ ligand can function as a nucleophile. The combination of these data with previously reported stopped-flow, kinetic, and X-ray crystallographic data allows a novel catalytic mechanism to be proposed for NHase enzymes with a heretofore unknown role for the $\alpha\text{Cys}^{113}\text{-OH}$ sulfenic acid ligand (Figure 4).^{11,26–28}

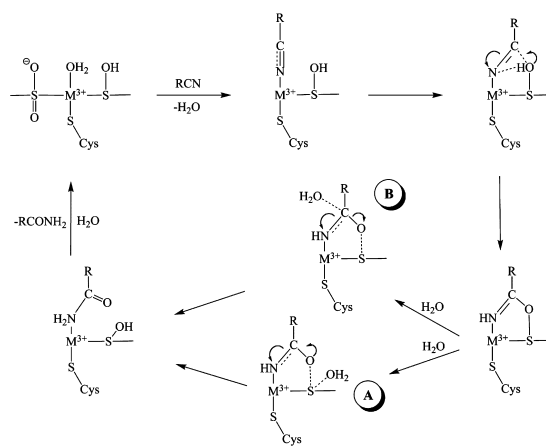


Figure 4. Proposed catalytic mechanism for NHase.

Stopped-flow data indicate that the first step in catalysis involves the direct ligation of the nitrile to the active site low-spin, trivalent metal ion.¹¹ Displacement of the metal-bound water molecule by a nitrile and coordination to the active site metal center activates the CN bond toward nucleophilic attack by the $\alpha\text{Cys}^{113}\text{-OH}$ sulfenic acid ligand. Once nucleophilic attack of the nitrile carbon occurs, two protons are transferred in the rate-limiting step for both Fe- and Co-type NHase enzymes.^{28,29} We propose that one proton transfer occurs between the $\alpha\text{Cys}^{113}\text{-CH}$ ligand and the nitrile N-atom, while the second transfer occurs between the water molecule that reforms $\alpha\text{Cys}^{113}\text{-OH}$ and the newly forming imidate N-atom, consistent with the observed normal isotope effect.^{28,29} That the $\alpha\text{Cys}\text{-OH}$ ligand is protonated was suggested by S K-edge XAS and DFT studies.¹⁹ Once proton transfer occurs, the

resulting covalently bound imidate can tautomerize to form an amide upon nucleophilic attack by a water molecule on αCys^{113} (pathway A). Alternatively, nucleophilic attack by water at the C-atom of the imidate intermediate could occur (pathway B), such that the O-atom of the amide product would be derived from H_2O , not the sulfenic group. In this alternative, the Co(III) ion and sulfenic acid group work together to form and stabilize the imidate intermediate, which can then be hydrated with sulfenic acid functioning as the leaving group. Finally, the amide product can be displaced by a water molecule and thus provide the regenerated catalyst.

■ ASSOCIATED CONTENT

Supporting Information

A detailed description of the materials, methods, kinetic analysis, and X-ray data collection and refinement, along with supplementary figures. This material is available free of charge via the Internet at <http://pubs.acs.org>. The reported coordinates and structure factors have been deposited in the PDB bank as Native P tNHase (PDB code: 4OB3), P tNHase -BuBA Co-crystal (PDB code: 4OB1), P tNHase -BuBA soaking (PDB code: 4OB2), and P tNHase -PBA Co-crystal (PDB code: 4OB0).

■ AUTHOR INFORMATION

Corresponding Author

richard.holz@marquette.edu

Author Contributions

[†]S.M. and R.W. contributed equally.

Notes

The authors declare no competing financial interest.

■ ACKNOWLEDGMENTS

The authors thank Dr. Miguel Ballicora for helpful discussions on enzyme kinetics. This work was supported by the National Science Foundation (CHE-1058357, RCH). GM/CA @ APS has been funded in whole or in part with Federal funds from the National Cancer Institute (Y1-CO-1020) and the National Institute of General Medical Sciences (Y1-GM-1104). Use of the Advanced Photon Source was supported by the U.S. Department of Energy, Basic Energy Sciences, Office of Science, under Contract No. DE-AC02-06CH11357.

■ REFERENCES

- (1) Yamada, H.; Kobayashi, M. *Biosci. Biotech. Biochem.* **1996**, *60*, 1391.
- (2) Brady, D.; Beeton, A.; Zeevaert, J.; Kgaje, C.; van Rantwijk, F.; Sheldon, R. A. *Appl. Microbiol. Biotechnol.* **2004**, *64*, 76.
- (3) Huang, W.; Jia, J.; Cummings, J.; Nelson, M.; Schneider, G.; Lindqvist, Y. *Structure* **1997**, *15*, 691.
- (4) Nagashima, S.; Nakasako, M.; Dohmae, N.; Tsujimura, M.; Takio, K.; Odaka, M.; Yohda, M.; Kamiya, N.; Endo, I. *Nat. Struct. Biol.* **1998**, *5*, 347.
- (5) Miyanaga, A.; Fushinobu, S.; Ito, K.; Wakagi, T. *Biochem. Biophys. Res. Commun.* **2001**, *288*, 1169.
- (6) Brodtkin, H. R.; Novak, W. R. P.; Milne, A. C.; D'Aquino, J. A.; Karabacak, N. M.; Goldberg, I. G.; Agar, J. N.; Payne, M. S.; Petsko, G. A.; Ondrechen, M. J.; Ringe, D. *Biochemistry* **2011**, *50*, 4923.
- (7) Kovacs, J. A. *Chem. Rev.* **2004**, *104*, 825.
- (8) Petrillo, K. L.; Wu, S.; Hann, E. C.; Cooling, F. B.; Ben-Bassat, A.; Gavagan, J. E.; Dicosimo, R.; Payne, M. S. *Appl. Microbiol. Biotechnol.* **2005**, *67*, 664.
- (9) Prasad, S.; Bhalla, C. *Biotechnol. Adv.* **2010**, *28*, 725.
- (10) Baxter, J.; Cummings, S. P. *Antonie van Leeuwenhoek* **2006**, *90*, 1.

(11) Gumataotao, N.; Kuhn, M. L.; Hajnas, N.; Holz, R. C. *J. Biol. Chem.* **2013**, *288*, 15532.

(12) Morrison, J. F.; Walsh, C. T. In *Advances in Enzymology and Related Areas of Molecular Biology*; John Wiley & Sons, Inc.: 2006; p 201.

(13) Baker, J. O.; Wilkes, S. H.; Bayliss, M. E.; Prescott, J. M. *Biochemistry* **1983**, *22*, 2098.

(14) Springsteen, G.; Wang, B. *Tetrahedron* **2002**, *58*, 5291.

(15) Liu, C. T.; Benkovic, S. J. *J. Am. Chem. Soc.* **2013**, *135*, 14544.

(16) DePaola, C. C.; Bennett, B.; Holz, R. C.; Ringe, D.; Petsko, G. A. *Biochemistry* **1999**, *38*, 9048.

(17) Smoum, R.; Rubinstein, A.; Dembitsky, V. M.; Srebnik, M. *Chem. Rev.* **2012**, *112*, 4156.

(18) Miyanaga, A.; Fushinobu, S.; Ito, K.; Shoun, H.; Wakagi, T. *Eur. J. Biochem.* **2004**, *271*, 429.

(19) Dey, A.; Chow, M.; Taniguchi, K.; Lugo-Mas, P.; Davin, S.; Maeda, M.; Kovacs, J. A.; Odaka, M.; Hodgson, K. O.; Hedman, B.; Solomon, E. I. *J. Am. Chem. Soc.* **2006**, *128*, 533.

(20) Murakami, T.; Nojiri, M.; Nakayama, H.; Odaka, M.; Yohda, M.; Dohmae, N.; Takio, K.; Nagamune, T.; Endo, I. *Protein Sci.* **2000**, *9*, 1024.

(21) Tsujimura, M.; Odaka, M.; Nakayama, H.; Dohmae, N.; Koshino, H.; Asami, T.; Hoshino, M.; Takio, K.; Yoshida, S.; Maeda, M.; Endo, I. *J. Am. Chem. Soc.* **2003**, *125*, 11532.

(22) Arakawa, T.; Kawano, Y.; Katayama, Y.; Nakayama, H.; Dohmae, N.; Yohda, M.; Odaka, M. *J. Am. Chem. Soc.* **2009**, *131*, 14838.

(23) Heinrich, L.; Mary-Verla, A.; Li, Y.; Vaissermann, J.; Chottard, J.-C. *Eur. J. Inorg. Chem.* **2001**, 2203.

(24) Heinrich, L.; Li, Y.; Vaissermann, J.; Chottard, J.-C. *Eur. J. Inorg. Chem.* **2001**, 1407.

(25) Yano, T.; Wasada-Tsutsui, Y.; Arii, H.; Yamaguchi, S.; Funahashi, Y.; Ozawa, T.; Masuda, H. *Inorg. Chem.* **2007**, *46*, 10345.

(26) Hashimoto, K.; Suzuki, H.; Taniguchi, K.; Noguchi, T.; Yohda, M.; Odaka, M. *J. Biol. Chem.* **2008**, *105*, 15334.

(27) Yamanaka, Y.; Hashimoto, K.; Ohtaki, A.; Noguchi, K.; Yohda, M.; Odaka, M. *J. Biol. Inorg. Chem.* **2010**, *15*, 655.

(28) Mitra, S.; Holz, R. C. *J. Biol. Chem.* **2007**, *282*, 7397.

(29) Rao, S. N.; Holz, R. C. *Biochemistry* **2008**, *47*, 12057.